Impacts of GIC on the New Zealand gas pipeline network

M. Ingham[1], T. Divett[1], C.J. Rodger[2] and M. Sigley[3]

[1]School of Chemical and Physical Sciences, Victoria University of Wellington, Wellington, New Zealand.

[2]Department of Physics, University of Otago, Dunedin, New Zealand.

[3]First Gas Ltd., New Plymouth, New Zealand.

Corresponding author: Malcolm Ingham (malcolm.ingham@vuw.ac.nz)

Key Points:

- Variations in cathodic protection (CP) monitoring data on the New Zealand gas pipeline network during geomagnetic storms are reported.
- Three locations are identified as having variations which suggest that during large storms the level of CP may be compromised.
- At any location the CP system responds to electric fields across the whole pipeline network and not to local electric field orientation.

Abstract

Geomagnetically induced currents (GIC) produced during geomagnetic storms present a potential risk to gas pipeline systems by disturbing the cathodic protection (CP) systems used to protect the pipeline from corrosion. In this study we look at CP monitoring data from a number of sites on the gas pipeline network in the North Island of New Zealand. We focus on variations during geomagnetic storms in three aspects of the CP system: 1) the output voltage of the constant current rectifiers, 2) the potential between the pipe and a $Cu/CuSO_4$ reference cell, and 3) the potential between an installed metal coupon and the reference cell. The industry standard for suitable CP is that the latter potential should lie between -0.85 V and -1.2 V when the rectifier is momentarily turned off. Three monitoring sites in particular are identified as showing very large variations in rectifier output voltage during geomagnetic storms, suggesting a possible risk to the system at these sites. Additionally, one of the three sites has coupon potentials which appear to rise above the -0.85 V level. Magnetotelluric (MT) impedance data are used to assess how effects at the monitoring sites relate to the magnitude and direction of induced electric fields. It clear that the response at any monitoring site is related to effects on the pipeline network as a whole. We also note the risks of disbonding and hydrogen induced cracking, issues we do not believe have been widely recognized in the research community.

Plain Language Summary

Variations in Earth's magnetic field during geomagnetic storms induce electric currents (geomagnetically induced currents – GIC) in the ground which, in certain circumstances, may disrupt the cathodic protection systems used to protect buried gas pipelines from corrosion. In this study we examine monitoring data from the cathodic protection system on the gas pipeline network in the North Island of New Zealand to assess where GIC may present a possible threat to the integrity of the network. We identify four locations where significant variations in monitoring data occur in response to geomagnetic field variations and where additional monitoring is desirable. There appears to be a potential risk to the pipeline system at these sites. It is apparent that the complex geology and tectonics of New Zealand has a major influence on how GIC affect the pipeline network.

1 Introduction

Variations in the geomagnetic field resulting from the interaction of the solar wind with Earth's magnetosphere and ionosphere induce electric fields in the conducting Earth. The induced currents (geomagnetically induced currents or GIC) can have significant effects on ground-based technological systems (Boteler et al., 1998; Pirjola, 2002). The impact of GIC on power transmission networks has been, and continues to be, studied in many countries and regions. Recent studies include those in China (Liu et al., 2018), Sweden and the wider Scandinavian region (Myllys et al. 2014; Rosenqvist and Hall, 2019; Sokolova et al., 2019), Austria (Bailey et al., 2017, 2018), Italy (Tozzi et al., 2019), Spain (Torta et al., 2014, 2017), France (Kelly et al., 2017), the United Kingdom (Beggan et al., 2013), New Zealand (Divett et al., 2017, 2018, 2020; Mac Manus et al., 2022), and the United States (Love et al., 2018).

GIC also present a risk to the cathodic protection (CP) systems that protect long pipelines from corrosion. Gideon (1971) and Campbell (1978, 1980) were the first to investigate such effects, on the Alaska pipeline. Further studies have since taken place in Argentina (Osella et al., 1998), Australia (Marshall et al., 2010, 2013), Canada (Fernberg et al., 2007), and extensively on the Finnish pipeline network (Viljanen, 1989; Pulkkinen et al., 2001a; Pirjola et al., 2003; Viljanen et al., 2006, 2010; Hajra,2022). Modelling of such effects using distributed source transmission-line (DSTL) theory or pi-networks has been described by, amongst others, Boteler (2000, 2013) and Pulkkinen et al., (2001b) and follows early work by Taflove & Dubowski (1979) and Dubowski & Taflove (1979) who investigated and modelled voltages in pipelines produced by inductive coupling with 60 Hz powerlines which shared the same right of way. In the context of GIC, in addition to direct induction in a pipeline by variations in the geomagnetic field, modern modelling techniques also allow for the effects of currents induced in the ground passing onto and off the pipeline through the insulating coating. In both cases it is assumed that effects are related to an induced electric field which is parallel to the pipeline.

Ingham & Rodger (2018) reported electric and magnetic field measurements made 25 years earlier at a single location on a gas pipeline in New Zealand. Correlations were drawn between these measurements and variations in the measured potential between the pipe and a nearby reference cell. A major conclusion of this study was that contrary to expectation the pipe to soil potential appeared to be most sensitive to local electric field variations which were perpendicular to the pipe. This was inferred to be related to the fact that the pipe was essentially parallel to the nearby coastline and that electric field variations were largely controlled by the coastal conductivity contrast.

In the present study we look more widely at the impact of geomagnetic storms on the high-pressure gas pipeline network in New Zealand, focussing on three branches of the network. To do this we use monitoring data supplied by the pipeline operators, First Gas Limited. We first give a brief outline of the monitoring of the CP system used on the New Zealand pipeline network. This is followed by a description of that network and the data availability. In sections 3 and 4 we discuss actual monitoring data as recorded during various periods of geomagnetic activity and attempt to identify sections of the pipeline network which may be most at risk from GIC. We finish by suggesting avenues for further work based on this assessment and some discussion of the issue of "disbonding" of a pipeline coating from the pipe, something which to date has received little or no previous attention from those in the space weather community researching the effects of GIC on pipelines but has been identified by the First Gas CP engineers as an area of significant interest.

2 Cathodic protection monitoring of the New Zealand pipeline network

2.1 Cathodic protection

The aim of cathodic protection (CP) is to prevent corrosion of a steel pipe which may occur when the pipe is exposed in an aerated but neutral electrolyte. In this circumstance, as explained by Wagner & Traud (2006), iron in the pipe is oxidized to Fe^{2+} and current passes from the pipe to the surrounding ground. To prevent corrosion, it is necessary to maintain the pipe at a negative potential of between -0.85 and -1.2 V with respect to the ground (Popov & Lee, 2018). The maximum level of -0.85 V is deemed as generally sufficient to prevent the pipe from becoming positive with respect to ground. Large variations which allow the pipe to become more negative than -1.2 V with respect to ground may lead to "disbonding" – the loss of adhesion between the insulating coating and the pipe. This results from the formation of hydroxyl ions at the metal surface (Latino et al., 2016) and is discussed further below. In an impressed current CP system protection is achieved by using a series of rectifiers and associated anode beds to keep the pipeline at the required negative potential. The actual level of CP can be measured using the kind of arrangement shown by Gummow (2002), represented schematically in Figure 1. This involves the installation near the pipe of a small metal coupon which is electrically connected to the pipe. The potential of both the pipe and the coupon relative to a $Cu/CuSO_4$ half-cell are measured. Whilst the rectifier is turned on the potential between the pipe and reference cell is the sum of three potentials – the polarization potential at the pipe/soil interface, the potential drop due to the resistance of the ground between the rectifier and the pipe, and any additional potential due to GIC. When the rectifier is intermittently turned off the effect of the potential drop in the ground is removed from the pipe to reference cell potential but the effect of GIC and the polarization potential remain. However, if the connection of the coupon to the pipe is simultaneously interrupted, this removes not only the effect of the rectifier from measurement of the coupon-reference cell potential but also any influence on this potential due to GIC. Thus the instantaneous "rectifier-off" potential gives a good estimate of the pipe/soil polarization potential i.e. the level of cathodic protection. More specifically, variations in the coupon-reference cell potential of more than 0.35 V when the rectifier is off indicates that the CP may move outside the "safe" region of -0.85 to -1.2 V. Further information on how seneitive the CP system is to geomagnetic field variations is given by monitoring the rectifier output voltage and current as well as the potential between the pipe itself and the $Cu/CuSO_4$ reference cell.

Shown in Figure 2 is an example of such monitoring data from one location on the New Zealand pipeline network during a relatively minor magnetic storm on 1 September 2019. Although the maximum value of K_P reached 6-, for most of this day the level was about 5, indicating a minor geomagnetic disturbance. Measurements are made every second. The periodic interruption of the constant current rectifier is shown by the spikes on all four traces when the rectifier current goes to zero.

The variations in the magnetic field induce electric fields in the pipe and in the Earth which cause the potential of the pipe to change. For example, in the period between 0600 and 1200 UT the potential of the pipe relative to the reference cell decreases significantly several times over a short time interval, as seen in the third panel of Figure 2. In each case this can be regarded as the pipe becoming more negative relative to the surrounding ground. As the rectifier output voltage is essentially the potential difference between the anode bed and the pipe, this means that the pipe is becoming more negative relative to the (distant) anode bed and the rectifier voltage, i.e. the potential between the anode bed and the pipe, increases (upper panel of Figure 2). Conversely, as the pipe to reference cell potential becomes less negative the rectifier output voltage decreases.

Given the proximity of the coupon to the pipe, changes in the potential between the coupon and the reference cell while the rectifier is on tend to follow those in the pipe to reference cell potential. However, the "rectifier-off" potential between the coupon and the reference cell, which shows the level of cathodic protection, essentially remains constant. In the case shown in Figure 2 this is at a value of around -1.2 V, indicating that the pipe is suitably protected throughout this geomagnetically disturbed time period. Except for short periods when the rectifier output voltage is changing rapidly the current supplied to the pipe by the rectifier remains constant at around 100 mA, which is expected as the rectifiers are constant current devices.

2.2 The New Zealand pipeline network

The gas transmission network in the North Island of New Zealand, operated by First Gas Limited, is shown in Figure 3, along with the naming of important regions (in italics) and cities (in capital letters). Most gas production is from offshore fields close to Taranaki and the major part of the high-pressure transmission network runs north and south from here to the major cities of Auckland and Wellington respectively. From this main pipeline branches run east to Gisborne (also serving the Bay of Plenty) and Napier, with a line also extending north from Auckland to Whangarei. The network consists of 48 rectifier sites with anode beds to provide impressed current cathodic protection and, additionally, a number of locations with earthing electrodes. Rectifier sites have active monitoring of a combination of the rectifier voltage and current, the potential difference between the pipe and a ($Cu/CuSO_4$) reference electrode, and the potential difference between a metal coupon and the reference electrode. In this work we focus on 10 sites which cover the three branches of the pipeline to Northland, Gisborne/Bay of Plenty and Napier. Of the 10 sites, 5 (Jack Henry Road, Tumunui Block, Okaro Road, Waimana Road and Whatatutu Road) are on the west-east pipeline which serves the Bay of Plenty, two (Watershed Road and Raukawa Road) are on the west-east pipeline that serves Hawkes Bay and three (Salle Road, Waipu Cove Road and Amriens Road) are on the pipeline which extends north from Auckland to Whangarei. The data from these sites were provided by First Gas on the grounds that they were felt likely to be "interesting" to examine in the space weather context.The data from these sites were provided by First Gas on the grounds that they were felt likely to be "interesting" to examine in the space weather context.

2.3 Data availability

To assess the general response of these branches of the New Zealand gas pipeline network to geomagnetic variations the monitoring data covering ten magnetic storms between November 2017 and October 2020 have been studied. The time spans bracketing these storms is given in Table 1, while the availability of the different types of monitoring data at each site during the storms is shown in Table 2. In some cases there are changes in the types of monitoring data available between events for the same location. As the overall time span studied falls largely in the solar minimum between solar cycles 24 and 25 maximum K_p values for the storms shown, as can be seen from Table 1, lie only between 5- and 7+, with only one storm reaching the latter level. Also, as seen in Table 2, the full suite of monitoring data (i.e. rectifier voltage and current, pipe to reference cell potential, and coupon to reference cell potential) is only available at a small number of the monitoring locations. In some cases measurements of the coupon to reference cell potential include the voltage drop in the cable connecting the rectifier to the coupon and therefore give a slightly more negative potential than actually exists between the coupon and reference cell. At most monitoring sites, in the most recent data, the rectifier is turned off every 5 to 10 minutes, although at Amriens Road and Watershed Road this interval is 6 hours.

3 Monitoring data

In the following two sections we look at the different kinds of monitoring data from a selection of the storms listed in Table 1. We start by surveying the most widely recorded set of monitoring data – measurements of the rectifier output voltage – before looking at variations in pipe and coupon to reference cell data.

3.1 Rectifier output voltage variations

Shown in Figure 4 are the horizontal magnetic field variations measured at the Eyrewell (EYR) geomagnetic observatory over a 4-hour period at the peak of the K_P max = 7+ geomagnetic storm on 26 August 2018 (storm 2 in Table 1). The Eyrewell observatory is part of the Intermagnet network and is located just to the north of Christchurch in New Zealand's South Island, and is the only New Zealand geomagnetic observatory. One-second measurements from EYR are therefore the only magnetic field data available from New Zealand which can be compared to the variations in CP monitoring data. During this storm, over a period of about 40 minutes, there were variations of nearly 500 nT in both the northward (B_x) and eastward (B_y) components of the magnetic field. Although variations over the North Island are probably slightly smaller, as suggested by Divett et al. (2020) the field as measured at EYR can be regarded as a good approximation to variations further north.

Variations in the rectifier output voltage at 9 of the 10 monitoring sites are available for this time period and are shown in Figures 5-7. The monitoring sites shown are the three on the section of pipe north of Auckland (Salle Road – SR, Waipu Cove Road – WCR, Amriens Road – AR), the two monitoring sites on the section of pipeline serving Hawkes Bay (Watershed Road – WtR, Raukawa Road – RR) and four of the monitoring sites on the Bay of Plenty/Gisborne section of pipe (Jack Henry Road – JHR, Tumunui Block – TB, Okaro Road – OR, Waimana Road – WaR).

To the north of Auckland (Figure 5) very large variations in rectifier output occur at Salle Road and Waipu Cove Road. At Salle Road, starting from about 0630 UT, the output voltage first rises from about 3 V to 5 V before dropping to 1 V at 0722 and then rising to a peak of nearly 8.5 V at around 0745. The voltage subsequently drops to around 1 V again before variations gradually die away with a series of oscillations. At Waipu Cove Road the variations are even more extreme reaching a peak of nearly 10 V and actually becoming negative around both 0722 and 0805 UT. Such extreme variations clearly suggest that GIC are having a major impact on the CP system at these locations.

At Amriens Road monitoring site, just to the north of Auckland and some 100 km south of Salle Road and Waipu Cove Road, the variations in rectifier output are both much smaller and 180° out of phase compared to those from the sites to the north. As discussed by Boteler & Seager (1998) such a phase reversal is expected between ends of a pipeline terminated by insulating flanges. However, that explanation for phase reversals is not applicable in this instance as in the New Zealand network, apart from a single disconnect near New Plymouth between the northern and southern parts of the network, the pipeline is electrically continuous with conducting connections across all insulating flanges. As is apparent from Figure 3 there are also no earthing points on the pipeline between Waipu Cove Road and Amriens Road which might explain the phase reversal. A possible rationale may lie in the parallel, but separate, pipeline from an oil refinery near Whangarei which for CP reasons is bonded to the First Gas network. The difference in magnitude of potential variations is likely to result from a combination of the existence of a non-uniform electric field parallel to the pipeline and the different distances of the sites relative to the ends of the pipeline segments or earthing points.

Variations in rectifier output for the same time period for four monitoring sites on the section of pipeline that runs to the Bay of Plenty and Gisborne are shown in Figure 6. Along this section of pipeline there are a significant number of earthing beds (grey dots in Figure 3) and it seems clear that these have a major effect on the CP response. This is most noticeable at Jack Henry Road (JHR) where there is practically no variation in rectifier voltage output during the storm. Immediately to the north of Jack Henry Road are several earthing beds which mean that the pipe potential must be very closely tied to ground such that any GIC flowing on to or off the pipe along its length to the east of JHR do not result in potential changes. The almost uniformly high rectifier output of between 34-35 V probably results from extremely high ground resistance, associated with the location of this site on or close to the 320-340 ka ignimbrites of the Whakamaru formation (Wilson et al., 1986), requiring a high rectifier voltage to supply the necessary cathodic protection current.

Tumunui Block (TB) and Okaro Road (OR) are only some 6-7 km apart and show very similar magnitude variations in rectifier output. The two sites do, however, sit on different pipeline segments with Tumunui Block situated on a northern branch of pipeline which extends from the main Gisborne line towards the city of Rotorua, while Okaro Road is on the main pipeline branch. Again, an earthing bed just to the south, on the pipeline branch going south to Taupo, may be responsible for the muted variations (relative to those at Salle Road and Waipu Cove Road). It is possibly also pertinent that the two sites sit almost midway between the earthing beds to the north of JHR in the west and a single earthing bed a similar distance away to the east (Figure 3). As discussed by Pulkkinen et al. (2001b), in the case of a uniform electric field parallel to a long pipeline GIC effects on pipe-to-soil potential should be minimal midway along the pipe. Also notable is the fact that the peak disturbance in rectifier output at these two sites occurs at about 0730 UT which is significantly earlier than at the three sites north of Auckland. This may well reflect the complexity of the pipeline response as, as discussed further below, induced electric field orientations vary greatly across the North Island reflecting variations in geological/tectonic structure. Variations in rectifier output at Waimana Road (WaR) show both a general 180° phase difference from those at Tumunui Block and Okaro Road and a peak response which possibly occurs midway between the peaks at TB and OR and those at SR and WCR. The earthing bed to the east of OR lies between OR and Waimana Road so it seems unlikely that the phase reversal is related to being at opposite ends of a pipe segment.

Rectifier output voltages from the two monitoring sites on the section of pipeline to Hawkes Bay are shown in Figure 7. The muted variations at Watershed Road (WtR) are presumed to be related to the close proximity of earthing beds to both the west and east (Figure 3). Raukawa Road (RR) is much closer to the north-eastern end of the pipeline segment and shows a magnitude of voltage variations which is comparable to that seen at Salle Road and Waipu Cove Road. Indeed, as at WCR, the output voltage becomes negative for short periods of time around 0722 and 0805. Raukawa Road is approximately 70 km to the north-east of the location reported by Ingham & Rodger (2018) in their much earlier study on this segment of pipeline. Ingham & Rodger reported that significant variations in pipe to reference cell potentials were measured and were observed to become positive during periods of magnetic activity. Notwithstanding the existence of an earthing bed between RR and the location of the earlier study, it seems clear that this segment of pipeline remains susceptible to GIC.

As rectifier output data from the other monitoring site on the Bay of Plenty/Gisborne pipeline, Whatatutu Road (Figure 3), not available for August 2018, shown in Figure 8 are the Eyrewell horizontal magnetic fields and the rectifier output voltages for both Waimana Road and Whatatutu Road for an 8-hour period on 01 September 2019 (storm 8 in Table 1). This geomagnetic storm reached a K_P max of only 6- and was marked by a series of rapid variations in both horizontal components of the magnetic field (Figure 8 upper two panels).

Whatatutu Road is located between a series of earthing beds some 25 km to the north-west of Gisborne and shows similar magnitude variations in rectifier voltage as are seen at Waimana Road, although these show an apparent time lag behind the variations at Waimana Road. Interestingly, the variations in voltage at Whatatutu Road appear to closely follow the variations in the northward component of the magnetic field. However, the maxima also occur when B_y is changing most rapidly. Variations at Waimana Road do the opposite - follow, but are out of phase with, variations in B_y but show maxima when B_x is changing most rapidly. This again suggests an effect of the complexity of the orientation of induced electric fields across the North Island, in this case reflecting the fact that WhR lies on the relatively conductive sediments of the Hikurangi Margin along the east coast, but WaR lies close to, or on the more mountainous (and resistive) spine of the North Island.

Although data from only 2 of the magnetic storms listed in Table 1 are discussed above, analysis of the rectifier output monitoring data for all the listed storms suggests that the largest variations in rectifier output voltage occur consistently at Salle Road, Waipu Cove Road and Raukawa Road. This is illustrated in Table 3 which presents the mean value of the rectifier output voltage and its standard deviation for the listed time intervals taken for six of the storms listed in Table 1. These time intervals were selected as they each cover the period during which the largest fluctuations in the monitoring data were observed. Instances where the standard deviation exceeds 5% of the mean value are shown in bold in the table. This occurs for all of the listed storms at Waipu Cove Road and Raukawa Road and for four of the six at Salle Road. For the largest storm the standard deviation of the output voltage is greater than 55% of the mean value at Salle Road and Raukawa Road and exceeds the mean value at Waipu Cove Road. Raukawa Road and Waipu Cove Road are the two locations where, as discussed above, the rectifier voltage went negative during this storm. The standard deviation is also about 10% of the mean value at Amriens Road, while it is no larger than about 1% at any of the other sites. The same relative differences can be observed for the other storms shown in the Table. It is clear that if the variations in rectifier output voltage are to be taken as an indicator of the impact of GIC and locations along the pipeline network, then these four sites are by far the most at risk.

It also apparent from the lack of synchroneity of rectifier responses that the complex geological and tectonic structure of the North Island plays a major role in determining the impact of geomagnetic activity on the pipeline network.

3.2 Pipe to reference cell and coupon to reference cell voltages

Although variations in rectifier output voltage give a good idea of where the impact of GIC on the pipeline are most significant, the principal guide as to whether a section of pipeline is protected or not comes, as outlined previously, from the potential between the installed metal coupon and the Cu/$CuSO_4$ reference cell when the rectifier voltage is turned off. To provide corrosion protection this "rectifier-off" potential should be between -0.85 V and -1.2 V. Potentials more positive than -0.85V may allow the pipeline to corrode. Potentials more negative than -1.2V can produce hydroxyl ions that cause the coating to dis-bond from the pipe. If the potentials are very negative, free hydrogen can be produced, which can theoretically create cracks in the pipe steel.

Unfortunately, data for pipe to reference cell and coupon to reference cell potentials which are reliable across multiple sites are somewhat limited. The most appropriate example is for the most recent magnetic storm in Table 1 (storm 10) on 23-24 October 2020. This storm was only of K_P max 5-. The horizontal magnetic field variations measured at EYR over the 20-hour period from 1500 UT on 23 October to 1100 UT on 24 October are shown in Figure 9. Also shown for comparison with the variations in rectifier voltage shown in Figure 5 are the resulting variations in the rectifier output at Salle Road over this time interval. As can be seen the magnitude of changes in the rectifier output are only around 1 V, only 10-15% of the size of the changes seen during the much larger storm shown in Figure 5.

Shown in Figure 10 are the observed variations in the pipe to reference cell potential and the coupon to reference cell potential at the three monitoring sites to the north of Auckland. The pipe to reference cell potential variations at Salle Road show the behaviour discussed earlier in that increases in the rectifier output voltage are simultaneous with decreases in the pipe to reference cell potential. In other words, as the pipe becomes more negative with respect to ground the potential difference between the anode bed and the pipe (i.e. the rectifier output voltage) increases. This is most noticeable for the large decreases in pipe to reference cell potential at around 0330 and 0900 UT on 24 October (2730 and 3300 on the horizontal scale). Almost identical, but slightly larger variations are seen at Waipu Cove Road, while much smaller amplitude changes in pipe to reference cell potential occur at Amriens Road. Note also that, as for the rectifier output voltage variations, changes in pipe-to reference cell potential at Salle Road and Waipu Cove Road are in-phase, while those at Amriens Road are out of phase with the other two sites.

In contrast to the variations in pipe to reference cell potential, those in coupon to reference cell, while the rectifier is on, are of much lower amplitude. From the point of view of gauging the sufficiency of cathodic protection it is also clear that at Salle Road the “rectifier-off” potential is exceptionally stable at around -1.1 V, within the desired 0.35 V range of -0.85 to -1.2 V. At Waipu Cove Road the “rectifier-off” potential is also essentially stable but, in this case, at much closer to -1.2 V, at the limit of this range. Also of possible concern is the fact that at WCR, unlike at Salle Road, the “rectifier-on” coupon to reference cell potential varies such that at times it approaches or, for example at 2100 UT, becomes higher than the “stable” “rectifier-off” level. Given the relatively minor nature of geomagnetic activity shown in Figure 9 this raises the question of how the “rectifier-off” coupon to reference cell potential at WCR would behave in a much larger storm such as that shown in Figure 5. When the rectifier output voltage becomes very small, or even becomes negative, it suggests a situation where the “rectifier-off” coupon to reference cell potential may rise well above the desired maximum value of -0.85 V, or even in the worst-case scenario become positive. How negative the “rectifier-off” potentials come when there is a large increase in rectifier output is also of interest. Similar concerns exist for Amriens Road where the interval at which the rectifier is turned off is much longer, yet there are signs that the “rectifier-on” coupon potential may at times approach the stable “rectifier-off” value.

The only other two sites with comparable pipe and coupon to reference cell data are Waimana Road and Whatatutu Road on the Bay of Plenty/Gisborne segment of the pipeline. The data from these two sites for the same time period are shown in Figure 11. In both cases the variations in both pipe to reference cell and coupon to reference cell potentials are small and the “rectifier-off” values for the coupon to reference cell potential are stable and within the CP range.

4 Orientation of induced electric fields and pipeline response

Theoretical calculations of the response of a pipeline to geomagnetic activity are based on the premise that GIC result from electric fields induced in the ground in an orientation parallel to that of the pipeline (Pulkkinen et al., 2001b; Boteler, 2000, 2013). However, the resulting effect also depends on changes in direction of and branches in the pipeline, as well as variations in the conductance of the insulating coating. As can be seen from Figure 3 the New Zealand pipeline network has not only a relatively complex topology, including many small branches, but also has coatings of differing types and conductances on different segments.

Shown in Figure 12 is a simplified geological map of the North Island of New Zealand and it is apparent from this that the North Island pipeline network crosses several significant geological boundaries. As has been pointed out by Ingham & Rodger (2018) studies of the pipeline in Canada by Boteler et al. (2003) and Fernberg et al. (2007) showed that the largest variations in pipe to soil potential occurred where the pipeline crossed major terrane boundaries across which induced electric fields may vary significantly in both magnitude and direction.

A combination of a complex network topology which has varying physical properties and the existence of major geological boundaries may mean that GIC effects observed on the pipeline at one location may in fact be driven by induced fields some significant distance away. This may be particularly true for the Bay of Plenty line which leaves the main south-north pipeline to the south of Hamilton and then crosses both the Central Volcanic Region, where shallow electrical conductivity is generally quite high, the highly resistive greywacke of the Main Range, and then the conductive sediments of the Hikurangi Margin along the east coast. Crossing the Main Ranges at its narrowest point, the Hawkes Bay line generally lies in sediments along most of its length. Changes in the insulating coating of the pipe may also be an important factor with the main Wellington-New Plymouth-Auckland line having a coal tar coating while the Northland, Bay of Plenty/Gisborne and Hawkes Bay lines have more modern coatings with lower conductance.

In principle, the existence of magnetotelluric (MT) impedance data at a sufficient number of locations should allow the electric field at each location to be calculated for any magnetic field orientation, and using the magnetic field spectra for a given magnetic storm, also allow the time variation in the electric fields to be calculated. This would allow the distribution of electric fields, both in magnitude and orientation, to be correlated with the pipeline monitoring data and allow identification of specific parts of the pipeline where both the largest fields occur and where the fields are parallel to the local pipeline orientation. At present, MT data in the North Island of New Zealand are largely along the Hikurangi Margin and around the Central Volcanic Region with only a few sites outside these regions. However, shown in Figure 13 is an example of the type of analysis which may elucidate weaknesses in the pipeline network as more MT data are collected.

Shown on the map in the centre of Figure 13 are the MT-determined electric field arrows showing the magnitude and orientation of the field at 0745 UT on 26 August 2018. The electric fields are calculated from the MT impedance tensor at each site using the magnetic field variation as recorded at the Eyrewell geomagnetic observatory under the assumption that these are representative of magnetic field variations across New Zealand. As the top panel on the left side of the Figure shows, 0745 UT is the time at which the variation in the B_x component of the magnetic field measured at EYR reached its extreme value. Also shown are the rectifier output voltages at 5 of the monitoring sites. As can be seen, at this instant of time the orientation of the electric fields varied considerable from location to location. Although orientations were generally in a west to north-west direction along the southern part of the Hikurangi Margin (HM) and down the Main Ranges across to Taranaki, in the northern part of the HM fields were oriented more northerly, and in the Central Volcanic Region (CVR) tended west to south-west. There was also considerable variation in magnitude with fields of only ~ 50 mV/km on the HM and in the CVR, but much larger fields of several 100's mV/km elsewhere. Looking at specific locations it is also apparent that close to Raukawa Road, where the rectifier response was close to its maximum, the orientation of the small fields was close to perpendicular to the pipeline rather than parallel to it. This is essentially in agreement with the finding by Ingham & Rodger (2018) in their study. In contrast, electric fields close to Tumunui Block were significantly larger and oriented obliquely to the local pipeline orientation. These differences in orientation relative to the pipeline make it clear that the rectifier responses at these monitoring sites is almost certainly driven by the cumulative effect of electric fields across the entire pipeline network and not by purely local fields.

5 Discussion and summary

5.1 Summary of monitoring data

As indicated above, and shown in Table 3, analysis of the monitoring data for all the magnetic storms listed in Table 1 suggests that, of the monitoring sites studied, Salle Road, Waipu Cove Road and Raukawa Road are the sites most susceptible to the effects of GIC. Similarly, although recent coupon to reference cell data when the rectifier is off suggests that the pipeline at the three northern sites is suitably protected during minor geomagnetic activity, the observed occurrence of much larger variations in rectifier output voltage during larger magnetic storms (e.g. Figure 5) suggests that variations in CP potential may occur during these events. Further study is therefore desirable as during such an occurrence pipe to reference cell potentials may become positive, and coupon to reference cell potentials may rise above the desired maximum of -0.85 V. As the Auckland to Whangarei section of pipe predominantly runs south-north up the Northland peninsula it can be assumed that local electric fields induced by varying magnetic fields may be strongly polarized due to the influence of the coastlines to the east and west. However, there has to date been no direct measurement of induced electric fields and no magnetotelluric (MT) impedance data, which might be used to elucidate the orientation of induced fields, is available. Measurement of local induced electric fields along this section of pipeline is therefore a priority, and is now being planned for.

Analysis of the Bay of Plenty/Gisborne section of pipeline suggests that there are only small variations in rectifier output voltage and that "rectifier-off" coupon to reference cell potentials appear stable and in the appropriate range. It remains to be seen if this remains the case as geomagnetic activity increases during the rising part of Solar Cycle 25.

Given the lack of pipe or coupon to reference cell monitoring, the large rectifier output variations at Raukawa Road are a possible concern and suggest that detailed field measurements should be considered. It was also noted earlier that the study reported by Ingham & Rodger (2018) also indicated large variations in pipe to soil potential along the Hawkes Bay section of pipeline, the driving factor for which remains unknown.

5.2 Consideration of the Auckland to Wellington pipeline section

Thus far, variations at CP monitoring sites on the main part of the pipeline network between Wellington and Auckland have not been studied. This section of the pipeline runs largely adjacent to the coast and, as is common in a coastal environment, it is likely that during magnetic activity significant variations may occur in the horizontal component of the magnetic field which is perpendicular to the local coastline. This is essentially a result of the well documented "coast effect" long noted in studies of electromagnetic induction in the Earth (e.g. Parkinson, 1962; Parkinson & Jones, 1975; Fischer, 1979) and recently discussed in terms of its effect on GIC in power networks by Liu et al. (2018). As such variations are likely to induce electric fields perpendicular to the predominant magnetic field variations, these are likely to be parallel to the pipeline, giving the possibility that GIC effects on this lengthy section of pipe cannot be discounted. Additionally, the south-north section of pipeline to the south-east of New Plymouth runs very close, and parallel, to the Taranaki Fault which marks a zone of high electrical conductivity likely to channel currents (Stagpoole et al., 2009). As a precautionary approach, field measurements at two or three locations on this major pipeline section are desirable.

5.3 Space Weather, GIC, and pipeline coating disbanding

Much previous discussion of the effects of GIC on pipelines has centred on the possibility of corrosion if there is a defect in pipeline coating and geomagnetic activity causing the pipe to become positive with respect to ground. There has been little, if any, attention paid to the issue of disbonding of the pipe from its protective, insulating, coating. A simplified explanation is given by Larsen (2020), who quotes Wong (2015). In general pipeline coatings have a sufficiently high resistance that little current resulting from the application of cathodic protection actually passes through the coating on to the pipe. In the event of a defect in the coating (a "holiday" in industry terminology) the pipe is exposed in a limited way to the surrounding environment and current will reach the pipe through the defect. In this situation hydroxyl ions are produced by reactions at the surface of the pipe:

$$\tfrac{1}{2}\,O_2 + H_2O + 2e^- \rightarrow 2\,OH^-$$

$$2H_2O + 2e^- \rightarrow H_2 + 2\,OH^-$$

and can lead to the loss of adhesion between the pipe and the coating. The possibility for disbonding is increased if the coating is partly permeable to water and air, and if geomagnetic activity decreases the CP potential of the pipe such that the current on to the pipe increases. Once disbonding occurs the influx of water into the gap between pipe and coating exacerbates the situation. Breakdown of the coating then leads to increased risk of corrosion.

Also of concern is that hydrogen is produced at the pipe surface at pipe to soil potentials at or more negative than approximately -1.2V. In some circumstances this can cause elemental hydrogen to infiltrate pipeline steel, and may lead to hydrogen induced cracking of pipe steel (Cazenave et al., 2021).

In consequence, investigation of the effects of GIC on pipelines needs to consider not just the possibility of the pipe becoming more positive than -0.85V with respect to ground, but also becoming more negative than -1.2V with respect to ground.

As noted above, Space Weather researchers have traditionally considered the risk of enhanced corrosion in pipelines, while the disbonding and hydrogen induced cracking risks described above has not been widely recognized in the research community. In our communications about Space Weather hazards with First Gas CP engineering staff, it is clear that they consider the hazard posed by disbonding to be of similar importance as issues around potentially enhanced corrosion. We suggest that this is an important issue to draw to the attention of the wider Space Weather research community. In the context of the present study only data from the period between solar cycles 24 and 25 have been used and study of data from larger geomagnetic storms during cycle 25 will be beneficial in assessing the risk of disbanding.

Acknowledgments

This research was supported by the New Zealand Ministry of Business, Innovation and Employment Endeavour Fund Research Programme contract UOOX2002. The authors would like to thank First Gas Limited for supporting this study and allowing access to their monitoring data. Ted Betrand and Wiebke Heise of GNS Science, New Zealand are thanked for making available magnetotelluric data.

Data Availability Statement

Cathodic Protection monitoring data reported here are the property of First Gas New Zealand Ltd. Request for access to the data should be addressed in the first instance to Mark Sigley (mark.sigley@firstgas.co.nz). Magnetic observatory data from Eyrewell may be downloaded from www.intermagnet.org. The magnetotelluric impedance tensor data used in Figure 13 were collected by GNS Science, New Zealand. Requests for access should in the first instance be addressed to Wiebke Heise (W.Heise@gns.cri.nz).

References

Bailey, R.L., Halbedl, T.S., Schattauer, I., Römer, A., Achleitner, G., Beggan, C.D., Wesztergom, V., Egli, R. and Leonhardt, R. (2017). Modelling geomagnetically induced currents in midlatitude Central Europe using a thin-sheet approach. *Annales Geophysicae*, 35, 751-761, https://doi.org/10.5914/angeo-35-751-2017.

Bailey, R.L., Halbedl, T.S., Schattauer, I., Achleitner, G. and Leonhardt, R. (2018). Validating GIC models with measurements in Austria: evaluation of accuracy and sensitivity to input parameters. *Space Weather*, 16, 887-902, https://doi.org/10.1029/2018SW001842.

Beggan, C.D., Beamish, D., Richards, A., Kelly, G.S., & Alan, A.W. (2013). Prediction of extreme geomagnetically induced currents in the UK high-voltage network. *Space Weather*, 11 (7), 407-419, https://doi.org/10.1002/swe.20065.

Boteler, D.H. (2000). Geomagnetic effects on the pipe-to-soil potentials of a continental pipeline. *Advances in Space Research*, 26, 15-20.

Boteler, D.H. (2013). A new versatile method for modelling geomagnetic induction in pipelines. *Geophysical Journal international*, 193, 98-109, https://doi.org/10.1093/gji/ggs113.

Boteler, D.H., Pirjola, R.J. & Nevanlinna, H. (1998). The effects of geomagnetic disturbances on electrical systems at the earth's surface. *Advances in Space Research*, 22, 17-27.

Boteler, D. H., Trichtchenko, L., & Samson, C. (2003). Investigation of earth conductivity influence on pipe to soil potentials. Proceedings, NACE Northern Region, Eastern Conference, Ottawa, Sept 15-17, 2003.

Campbell, W. H. (1978). Induction of auroral zone electric currents within the Alaskan pipeline. *Pure and Applied Geophysics*, 116(6), 1143–1173.

Campbell, W. H. (1980). Observation of electric currents in the Alaskan oil pipeline resulting from auroral electrojet current sources. *Geophysical Journal of the Royal Astronomical Society*, 61(2), 437–449.

Cazenave, P., Jimenez, K., Gao, M., Moneta, A. & Hyreiuk, P. (2021). Hydrogen assisted cracking driven by cathodic protection operated at near -1200 mV CSE – an onshore gas pipeline failure. *Journal of Pipeline Science and Engineering*, 1, 100-121, https://doi.org/10.1016/j.jpse.2021.02.002.

Divett, T., Ingham, M., Beggan, C.D., Richardson, G.S., Rodger, C.J., Thomson, A.W., & Dalzell, M. (2017). Modeling geoelectric fields and geomagnetically induced currents around New Zealand to explore GIC in the South Island's electrical transmission network. *Space Weather*, 15 (10), https://doi.org/700 10.1002/2017SW001697.

Divett, T., Richardson, G.S., Beggan, C.D., Rodger, C.J., Boteler, D.H., Ingham, M., MacManus, D.H., Thomson, A.W.P. & Dalzell, M. (2018). Transformer-level modeling of geomagnetically induced currents in New Zealand's South Island. *Space Weather*, 16 (6), https://doi.org/708 10.1029/2018SW001814.

Divett, T., Mac Manus, D.H., Richardson, G.S., Beggan, C.D., Rodger, C.J., Ingham, M., Clarke, E., Thomson, A.W.P., Dalzell, M. & . Obana, Y. (2020). Geomagnetically induced current model validation from New Zealand's South Island. *Space Weather*, 18 (8), https://doi.org/704 10.1029/2020SW002494.

Dubkowski, J. & A. Taflove (1979). Prediction method for buried pipeline voltages due to 60 Hz AC inductive coupling. Part II – field test verification. IEEE Transactions on Power Apparatus and Systems, PAS-98, 788-794.

Fernberg, P. A., Samson, C., Boteler, D., Trichtenko, L., & Larocca, P. (2007). Earth conductivity structures and their effects on geomagnetic induction in pipelines. *Annales Geophysicae*, 25(1), 207–218.

Fischer, G. (1979). Electromagnetic induction effects at an ocean coast. In *Proceedings of the IEEE*, 67 (7), 1050-1060, https://doi: 10.1109/PROC.1979.11388.Gideon, D. N. (1971). Telluric current effects on buried pipelines. Materials Protection and Performance, 10, 5–10.

Gummow, R.A. (2002). GIC effects on pipeline corrosion and corrosion control systems. *Journal of Atmospheric and Solar-terrestrial Physics*, 64, 1755-1764.

Hajra, R. (2022). Intense, long-duration geomagnetically induced currents (GICs) caused by intense substorm clusters. *Space Weather*, 20, https://doi.org/10.1029/2021SW002937.

Ingham, M. & Rodger, C.J. (2018). Telluric field variations as drivers of variations in cathodic protection potential on a natural gas pipeline in New Zealand. *Space Weather*, 16, 1396-1409, https://doi.org/10.1029/2018SW001985.

Kelly, G.S., Viljanen, A., Beggan, C.D., & Thomson, A.W. (2017). Understanding GIC in the UK and French high-voltage transmission systems during severe magnetic storms. *Space Weather*, 15 (1), 99{114, https://doi.org/10.1002/2016SW001469.

Larsen, K.R. (2020). Using pipeline coatings with cathodic protection. *Materials Performance*, 4 May 2020, Accessed at https://www.materialsperformance.com/articles/cathodic-protection/2016/04/using-pipeline-coatings-with-cathodic-protection.

Latino, M., Varela, F., Tan, M..YJ. and Forsyth, M. (2016). An overview on cathodic shielding produced by disbonded coatings. In *Proceedings of the 2016 Corrosion and Prevention Conference*, Australasian Corrosion Association, Kerrimuir, Victoria, Paper 60.

Liu, C., Wang, X., Wang, H. and Zhao, H. (2018). Quantitative influence of coast effect on geomagnetically induced currents in power grids: a case study. *Journal of Space Weather and Space Climate*, 8, A60, https://doi.org/10.1015/swsc/2018046.

Love, J.J., Lucas, G.M., Kelbert, A., & Bedrosian, P. A. (2018). Geoelectric hazard maps for the Mid-Atlantic United States: 100-year extreme values and the 1989 magnetic storm. *Geophysical Research Letters*, 45 (1), 5-14, https://doi.org/728 10.1002/2017GL076042.

Mac Manus, D.H., Rodger, C.J., Ingham, M., Clilverd, M.A., Dalzell, M., Divett, T., Richardson, G.S. and Petersen, T. (2022).Geomagnetically induced current model in New Zealand across multiple disturbances, validation and extension to non-monitored transformers. *Space Weather*, 20, , 20, e2021SW002955, https://doi: 10.1029/2021SW002955.

Marshall, R. A., Gorniak, H., Van Der Walt, T., Waters, C.L., Sciffer, M.D., Miller, M., Dalzell, M., Daly, T., Pouferis, G., Hesse, G. & Wilkinson, P. (2013). Observations of geomagnetically induced currents in the Australian power network. *Space Weather*, 11, 6–16, https://doi.org/10.1029/2012SW000849.

Marshall, R.A., Waters, C.L., & Sciffer, D. (2010). Spectral analysis of pipe to soil potentials with variations of the Earth's magnetic field in the Australian region. *Space Weather*, 8, S05002, https://doi.org/10.1029/2009SW000553.

Myllys, M., Viljanen, A., Rui, Ø.A. and Ohnstad, T.M. (2014). Geomagnetically induced currents in Norway: the northernmost high-voltage power grid in the world. *Journal of Space Weather and Space Climate*, 4, A10, https://doi.org/10.1051/swsc/2014007.

Osella, A., Favetto, A., & Lopez, E. (1998). Currents induced by geomagnetic storms on buried pipelines as a cause of corrosion. *Journal of Applied Geophysics*, 38(3), 219–233.

Parkinson, W.D. (1962). The influence of continents and oceans on geomagnetic variations. *Geophysical Journal of the Royal Astronomical Society*, 6, 441–449.

Parkinson, W.D. and Jones, F.W. (1975). The geomagnetic coast effect. *Reviews of Geophysics and Space Physics*, 17, 1999–2015.

Pirjola, R. (2002). Review of the calculation of surface electric and magnetic fields and of geomagnetically induced currents in ground-based technological systems. *Surveys in Geophysics*, 23, 71-90.

Pirjola, R., Pulkkinen, A. & Viljanen, A. (2003). Studies of space weather effects on the Finnish natural gas pipeline and on the Finnish high-voltage power system. *Advances in Space Research*, 31, 795-805, https://doi.org/10.1016/S0273-1177(02)00781-0.

Popov, B.N. & Lee, J-W (2018). Cathodic protection of pipelines. In: Handbook of Environmental Degradation of Materials, editor Kurtz, M., pp 509-532, https://doi.org/10.1016/B978-0-323-52472-8.00023-3.

Pulkkinen, A., Viljanen, A., Pajunpää, K., & Pirjola, A. (2001a). Recordings and occurrence of geomagnetically induced currents in the Finnish natural gas pipeline network. *Journal of Applied Geophysics*, 48(4), 219–231.

Pulkkinen, A., Pirjola, A., Boteler, D., Viljanen, A. & Yegorov, I.(2001b). Modelling of space weather effects on pipelines. *Journal of Applied Geophysics*, 48(4), 233–256.

Rosenqvist, L. and Hall, J.O. (2019). Regional 3-D modelling and verification of geomagnetically induced currents in Sweden. *Space Weather*, 17, 27-36, https://doi.org/10.1029/2018SW002084.

Sokolova, E. Y., Kozyreva, O. V., Pilipenko, V. A., Sakharov, Y. A. and Epishkin, D. V. (2019). Space-weather-driven geomagnetic- and telluric-field variability in Northwestern Russia in correlation with geoelectrical structure and currents induced in electric-power grids. *Izvestiya, Atmospheric and Oceanic Physics*, 11, 1639-1658, https://doi.org/10.1134/S000143381911015X.

Stagpoole, V. M., Bennie, S. L., Bibby, H.M., Dravitzki, S. and Ingham, M.R. (2009). Deep structure of a major subduction back thrust: magneto-telluric investigations of the Taranaki Fault, New Zealand. *Tectonophysics*, 463, 77-85, https://doi.org/10.1016/j.tecto.2008.09.035.

Taflove, A. & J. Dubkowski, J. (1979). Prediction method for buried pipeline voltages due to 60 Hz AC inductive coupling. Part I – analysis. IEEE Transactions on Power Apparatus and Systems, PAS-98, 788-787.

Torta, J. M., Marsal, S. and Quintana, M. (2014), Assessing the hazard from geomagnetically induced currents to the entire high-voltage power network in Spain. *Earth Planets Space*, 66(1), 1–17, https://doi.org/10.1186/1880-5981-66-87.

Torta, J. M., Marcuello, A., Campanyà, J., Marsal, S., Queralt, P. and Ledo, J. (2017). Improving the modeling of geomagnetically induced currents in Spain. *Space Weather*, 15, 691–703, https://doi.org/10.1002/2017SW001628.

Tozzi, R., De Michelis, P., Coco, I. And Giannattasio, F. (2019). A preliminary risk assessment of geomagnetically induced currents over the Italian territory. *Space Weather*, 17, 46-58, https://doi.org/10.1029/2018SW002065.

Viljanen, A. (1989). Geomagnetically induced currents in the Finnish natural gas pipeline. *Geophysica*, 25, 135–159.

Viljanen, A., Pulkkinen, A., Pirjola, R., Pajunpää, K., Posio, P., & Koistinen, A. (2006). Recordings of geomagnetically induced currents and a nowcasting service of the Finnish natural gas pipeline system. *Space Weather*, 4, S10004, https://doi.org/10.1029/2006SW000234.

Viljanen, A., Koistinen, A, Pajunpää, K., Pirjola, R., Posio, P. &. Pulkkinen, A. (2010). Recordings of geomagnetically induced currents in the Finnish natural gas pipeline – summary of an 11-year period. *Geophysica*, 46(1-2), 59-67.

Wagner, C. & Traud, W. (2006). On the Interpretation of corrosion processes through the superposition of electrochemical partial processes and on the potential of mixed electrodes. *Corrosion*, 26(10), 844-855.

Wilson, C.J.N., Houghton, B.F. & Llyod, B.F. (1986). Volcanic history and eruption of the Maroa-Taupo area, Central North Island. In: Smith, I.E.M. (ed.) Late Cenozoic volcanism in New Zealand. *Royal Society of New Zealand Bulletin*, 23, 194-223.

Wong, D. (2015). Compatibility of pipeline coatings with cathodic protection. Protective Coating Technology Forum, CORROSION 2015, Dallas, Texas.

Figure captions

Figure 1: Schematic representation of CP monitoring station allowing measurement of "rectifier-off" potential between a metal coupon and a reference cell (after Gummow, 2002).

Figure 2: An example of CP monitoring data for a single day (1 September 2019) during which there was minor geomagnetic activity.

Figure 3: The First Gas pipeline network in the North Island of New Zealand. Red lines – pipelines coated with coal tar enamel; blue lines – pipelines with other, lower conductance, coatings; red dots – rectifier locations; grey dots – earthing electrodes; black dots – major cities/towns. Rectifier locations with CP monitoring which are discussed in this paper are named.

Figure 4: Variations in horizontal magnetic fields at EYR geomagnetic observatory during a 4-hour period from 0600 – 1000 UT on 26-08-2018.

Figure 5: Variations in rectifier output voltage over a 4-hour period from 0600 – 1000 UT on 26-08-2018 at the CP monitoring sites north of Auckland: Salle Road (SR), Waipu Cove Road (WCR), Amriens Road (AR). Locations are shown in Figure 3.

Figure 6: Variations in rectifier output voltage over a 4-hour period from 0600 – 1000 UT on 26-08-2018 at the CP monitoring sites along the Bay of Plenty section of pipeline: Jack Henry Road (JHR), Tumunui Block (TB), Okaro Road (OR), Waimana Road (WaR). Locations are shown in Figure 3.

Figure 7: Variations in rectifier output voltage over a 4-hour period from 0600 - 1000 on 26-08-2018 at the CP monitoring sites along the Hawkes Bay section of pipeline: Watershed Road (WtR), Raukawa Road (RR). Locations are shown in Figure 3.

Figure 8: Variations in in horizontal magnetic fields at EYR geomagnetic observatory and rectifier output voltages at Waimana Road (WaR) and Whatatutu Road (WhR) during an 8-hour period from 0600 - 1400 on 01-09-2019.

Figure 9: Variations in horizontal magnetic fields at EYR geomagnetic observatory during a 20-hour period from 1500 UT on 23-10-2020 to 1100 UT on 24-10-2020. The horizontal axis is marked as hours from 0000 UT 23-10-2020. Also shown is the variation in rectifier output voltage at Salle Road over this time interval.

Figure 10: Variations in pipe to reference cell potential (left column) and coupon to reference cell potential (right column) at Salle Road (SR), Waipu Cove Road (WCR) and Amriens Road (AR) over the 20-hour period from 1500 UT on 23-10-2020 to 1100 UT on 24-10-2020. The horizontal axis is marked as hours from 0000 UT 23-10-2020.

Figure 11: Variations in pipe to reference cell potential (left column) and coupon to reference cell potential (right column) at Waimana Road (WaR), and Whatatutu Road (WhR) over the 20-

hour period from 1500 UT on 23-10-2020 to 1100 UT on 24-10-2020. The horizontal axis is marked as hours from 0000 UT 23-10-2020.

Figure 12: Simplified geological map of the North Island of New Zealand.

Figure 13: Electric field orientations and magnitudes at 0745 UT on 28 August 2018 calculated from magnetotelluric (MT) impedance data. Also shown are the time variations in the magnetic field measured at EYR and the rectifier output voltage at 5 monitoring sites. The dashed horizontal lines on the rectifier output plots show the average value of the output over that day. The vertical red lines marking 0745 UT clearly show the shift in phase of the CP response at different monitoring sites.

Table captions

Table 1: Time periods around magnetic storms in 2017-2020 for which CP monitoring data have been studied in the current work.

Table 2: CP monitoring data availability for each of the 10 time periods listed in Table 1. R – rectifier voltage and current, P – pipe to reference cell potential, C – coupon to reference cell potential. Locations are shown in Figure 3.

Table 3: Mean values and standard deviations of variations in rectifier output voltage at all monitoring sites during specified time intervals of 6 of the storms listed in Table 1. Figures shown in bold represent occasions when the standard deviation of the variations exceeded 5% of the mean value.

Figure 1.


switch
V
$Cu/CuSO_4$
reference
electrode
Pipe
coupon

Figure 2.

Whatatutu Road
Rectifier output (V)
Rectifier current (mA)
Pipe to ref cell (V)
Coupon to ref cell (V)
3.5
3
2.5
2
1.5
150
100
50
0
-1
-1.5
-2
-2.5
0
6
12
18
24
UT (hrs) from 00 01-09-2019

Figure 3.

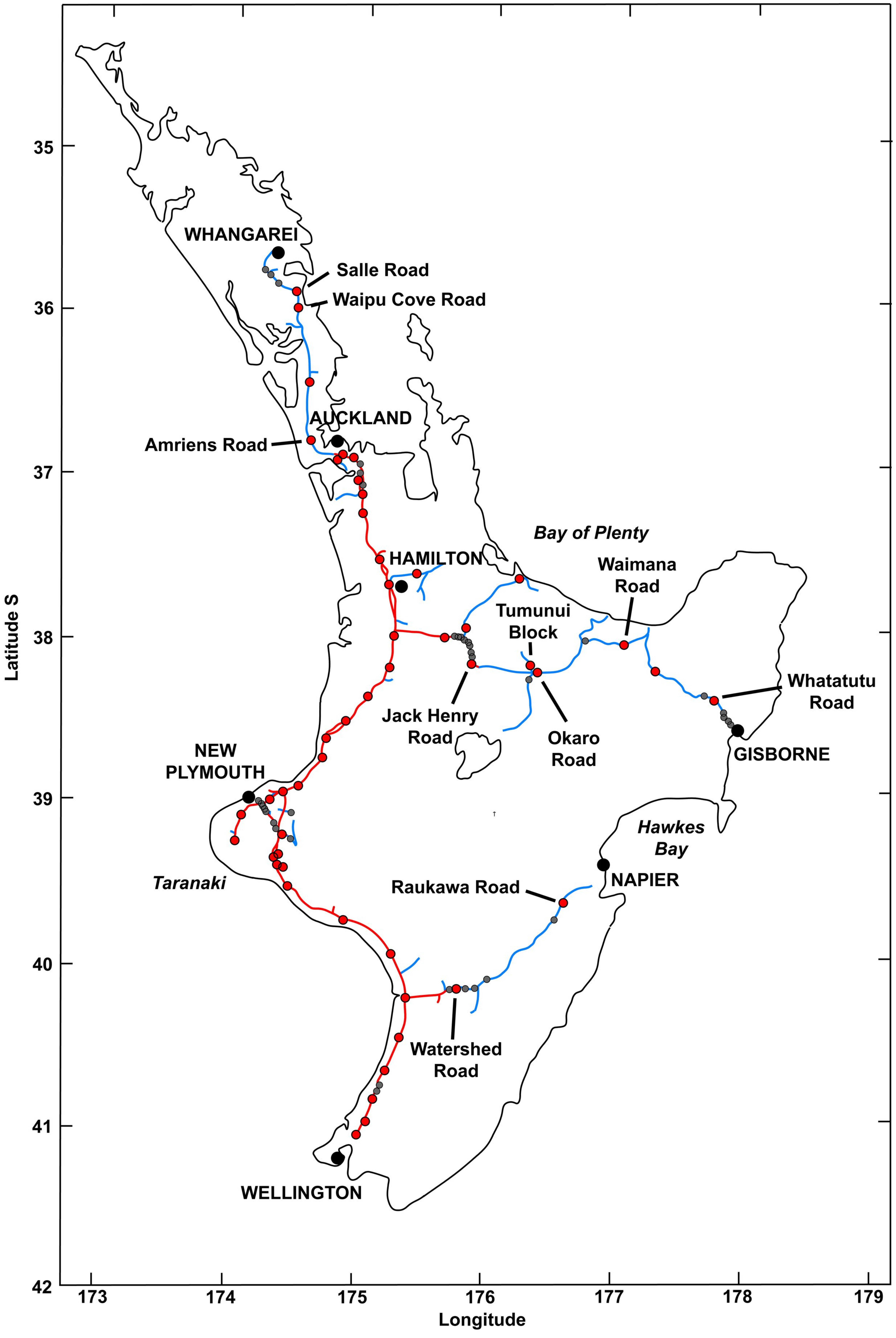
WHANGAREI
Salle Road
Waipu Cove Road
AUCKLAND
Amriens Road
Bay of Plenty
HAMILTON
Waimana Road
Tumunui Block
Jack Henry Road
Okaro Road
Whatatutu Road
GISBORNE
NEW PLYMOUTH
Hawkes Bay
NAPIER
Taranaki
Raukawa Road
Watershed Road
WELLINGTON
35
36
37
38
39
40
41
42
Latitude S
173
174
175
176
177
178
179
Longitude

Figure 4.


×10^4
1.95
1.94
1.93
1.92
1.91
1.9
EYR Bx (nT)
6
6.5
7
7.5
8
8.5
9
9.5
10
UT (hrs)
8500
8400
8300
8200
8100
8000
EYR By (nT)
6
6.5
7
7.5
8
8.5
9
9.5
10
UT (hrs)

Figure 5.

SR voltage (V)
WCR voltage (V)
AR voltage (V)
UT (hrs)
10
5
0
6
6.5
7
7.5
8
8.5
9
9.5
10

Figure 6.


JHR voltage (V)
35
34.5
34
TB voltage (V)
8
7
6
5
OR voltage (V)
4
3
2
1
WaR voltage (V)
8
6
4
6
6.5
7
7.5
8
8.5
9
9.5
10
UT (hrs)

Figure 7.


WtR voltage (V)
UT (hrs)
RR voltage (V)
UT (hrs)
8
6
4
2
0
6
6.5
7
7.5
8
8.5
9
9.5
10

Figure 8.

×10^4
EYR Bx (nT)
1.93
1.925
1.92
6
7
8
9
10
11
12
13
14
UT (hrs)
EYR By (nT)
8400
8350
8300
8250
UT (hrs)
WaR voltage (V)
5
4
3
2
UT (hrs)
WhR voltage (V)
4
3
2
1
UT (hrs)

Figure 9.


×10^4
1.93
1.9275
1.925
1.9225
1.92
1.9175
EYR Bx (nT)
15
18
21
24
27
30
33
UT (hrs)
8475
8450
8425
8400
8375
8350
8325
EYR By (nT)
UT (hrs)
6
4
2
0
SR voltage (V)
UT (hrs)

Figure 10.

SR pipe-ref voltage (V)
SR coupon-ref voltage (V)
WCR pipe-ref voltage (V)
WCR coupon-ref voltage (V)
AR pipe-ref voltage (V)
AR coupon-ref voltage (V)
UT (hrs)
0
-1
-2
-3
15
18
21
24
27
30
33

Figure 11.


WaR pipe-ref voltage (V)
WaR coupon-ref voltage (V)
WhR pipe-ref voltage (V)
WhR coupon-ref voltage (V)
0
-1
-2
-3
15
18
21
24
27
30
33
UT (hrs)

Figure 12.


Cenozoic/Cretaceous sediments
Jurassic/Triassic sediments
Cenozoic/Cretaceous volcanics
Greywacke
Whangarei
Auckland
Hamilton
Central Volcanic Region
New Plymouth
Gisborne
Napier
Main Ranges
Wanganui Basin
Hikurangi Margin
Wellington

Figure 13.

×10^4
EYR - Bx
EYR Bx (nT)
Time in hours 26-08-2018
EYR - By
EYR By (nT)
Time in hours 26-08-2018
TB Voltage (V)
Tumunui Block
Time in hours 26-08-2018
WtR Voltage (V)
Watershed Road
Time in hours 26-08-2018
Latitude S
Longitude
250 mV/km
Okaro Road
OR Voltage (V)
Time in hours 26-08-2018
Waimana Road
WaR Voltage (V)
Time in hours 26-08-2018
Raukawa Road
RR Voltage (V)
Time in hours 26-08-2018

Storm	**Date**	**K_P max**
1	2300 UT 06/11/2017 – 2300 UT 08/11/2017	6+
2	1200 UT 25/08/2018 – 1200 UT 27/08/2018	7+
3	1200 UT 10/09/2018 – 1200 UT 12/09/2018	6
4	1100 UT 04/11/2018 – 1100 UT 07/11/2018	6-
5	0000 UT 31/01/2019 – 1200 UT 01/02/2019	5+
6	1200 UT 13/05/2019 – 1200 UT 15/05/2019	6+
7	1200 UT 04/08/2019 – 1200 UT 06/08/2019	5+
8	1200 UT 30/08/2019 – 1200 UT 02/09/2019	6-
9	1200 UT 23/09/2020 – 1200 UT 29/09/2020	6-
10	1200 UT 23/10/2020 – 1200 UT 24/10/2020	5-

Table 1: Time periods around magnetic storms in 2017-2020 for which CP monitoring data have been studied in the current work.

Site/Storm	**1**	**2**	**3**	**4**	**5**	**6**	**7**	**8**	**9**	**10**
Salle Rd	R	RPC	RPC	RPC	RPC	RPC	RPC	RPC	RP	RPC
Waipu Cove Rd	R	R	R	R	R	R	R	RPC	RP	RPC
Amriens Rd	R	R	R		R	R	R	R	RPC	RPC
Jack Henry Rd	-	R	R	R	R	R	R	R	R	R
Tumunui Block	RP	RP	RP	RP	-	RP	RP	RP	-	-
Okaro Rd	-	R	R	-	R	R	R	R	R	R
Waimana Rd	R	R	R	RPC	RPC	RPC	RPC	RPC	RPC	RPC
Whatatutu Rd	-	-	-	RPC	RPC	RPC	RPC	RPC	RPC	RPC
Watershed Rd	R	R	R	R	R	R	R	R	R	R
Raukawa Rd	R	R	R	R	R	R	R	R	R	R

Table 2: CP monitoring data availability for each of the 10 time periods listed in Table 1. R – rectifier voltage and current, P – pipe to reference cell potential, C – coupon to reference cell potential. Locations are shown in Figure 3.

		0300-1800 UT 07/11/2017	0600-1200 UT 26/08/2018	0300-1200 UT 11/09/2018	0300-1100 UT 05/11/2018	0300-1000 UT 14/05/2019	0000-1200 UT 24/09/2020
K_P max		6+	7+	6	6-	6+	6-
Salle Rd	Mean	3.071	3.484	3.337	3.523	3.295	4.014
	SD	0.106	**2.179**	**0.351**	**0.342**	**0.438**	0.123
Waipu Cove Rd	Mean	2.315	2.379	2.223	2.406	1.967	2.529
	SD	**0.164**	**3.182**	**0.436**	**0.402**	**0.577**	**0.140**
Amriens Rd	Mean	4.571	4.406	4.529	4.459	4.646	4.194
	SD	0.021	**0.427**	0.053	0.043	0.066	0.021
Jack Henry Rd	Mean	-	-	34.52	-	44.11	41.48
	SD	-	-	-	-	-	0.055
Tumunui Bl	Mean	8.033	7.145	6.708	7.107	7.742	-
	SD	0.002	0.038	0.002	0.002	0.006	-
Okaro Rd	Mean	-	2.485	2.154	2.116	2.852	2.511
	SD	-	0.031	0.001	0.002	0.006	0.010
Waimana Rd	Mean	5.835	5.473	5.337	4.808	3.724	1.713
	SD	0.008	0.207	0.004	0.005	0.027	0.012
Whatatutu Rd	Mean	-	-	-	2.879	2.773	2.415
	SD	-	-	-	0.006	0.019	0.004
Watershed Rd	Mean	5.054	5.035	5.071	5.044	5.069	5.125
	SD	0.005	0.051	0.007	0.006	0.015	0.003
Raukawa Rd	Mean	3.242	3.252	3.255	3.386	3.328	3.500
	SD	**0.177**	**1.900**	**0.363**	**0.333**	**0.552**	**0.190**

Table 3: Mean values and standard deviations of variations in rectifier output voltage at all monitoring sites during specified time intervals of 6 of the storms listed in Table 1. Figures shown in bold represent occasions when the standard deviation of the variations exceeded 5% of the mean